

# The deterioration of sodium ion conductors under applied stress

KYOSHI KURIBAYASHI, PATRICK S. NICHOLSON

*Department of Metallurgy and Materials Science, McMaster University, Hamilton, Ontario, Canada*

Notched samples of two  $\beta''$ -aluminas and one NaZrPSiO were sodium-electrolysed at current densities up to  $2A\text{ cm}^{-2}$  under tensile and compressive bend stresses and uniaxial compression. Following electrolysis,  $K_{Ic}$  measurements were made in four-point-bend and reduction of this parameter taken as indicative of sample deterioration. In all cases, both tensile and compressive applied stresses during electrolysis enhanced deterioration suggesting the Poiseuille pressure model of deterioration is non-operable. An electrochemical corrosion model is suggested, involving the precipitation of sodium in the grain boundaries adjacent to current-focusing flaws by the oxidation of local oxygen ions. The observed influence of applied stress on deterioration is interpreted via relief of back-stresses resisting such sodium precipitation.

## 1. Introduction

The degradation of  $\beta$ - and  $\beta''$ - $\text{Al}_2\text{O}_3$  electrolytes in Na/S cells is one of the most important problems to be solved before such cells can be used for energy storage. Critical factors leading to electrolyte failure are the penetration of the electrolytes by molten sodium dendrites during charging and impurities such as  $\text{Ca}^{2+}$  and  $\text{K}^+$  [1, 2] in the molten sodium, sulphide or the cell container.

Armstrong *et al.* [3] first suggested that sodium ions were "focused" onto the tips of pre-existing sodium-filled cracks during the cell charging process. This localization of dischargant, they postulated, produced a stress in the crack arising from the developed Poiseuille pressure. This mechanism of degradation has been studied in detail by a number of authors [4-15]. Richman and Tennenhouse [4] proposed a "stress corrosion model" suggesting that the electrolyte "dissolves" at the crack tip, so extending the crack. This dissolution depends on the interaction of capillarity, the stress arising from the Poiseuille pressure and the selective removal of electrolyte from the crack tips by the effluxing sodium. Shetty *et al.* [6] and Davidge *et al.* [7] on the other hand, postulated a "critical fracture model"

in which crack extension only occurs when the stress-intensity at the crack-tips attains the critical value. Recently, slow degradation (called "Mode II" degradation [13]) was suggested involving the internal deposition of sodium in Na- $\beta$ - $\text{Al}_2\text{O}_3$  subjected to long term cycling in Na/S cells. The degradation via Poiseuille pressure (Mode I degradation) was suggested to be important in the initial stages of electrolyte degradation. In both cases, local current densities in the vicinity of crack tips will play a significant role. Since  $\beta$ - and  $\beta''$ - $\text{Al}_2\text{O}_3$  are anisotropic conductors (conductivity in the  $c$ -axis direction being  $\sim 10^7$  times lower than that in the conduction plane) the local current distribution in the ceramic will strongly depend on the microstructure. Further localizing factors are: (a) the fact that  $\beta$ - $\text{Al}_2\text{O}_3$  is not easily wetted by molten sodium [14, 16] and (b) possible back e.m.f.'s via pressurized sodium in flaws [10]. Uncertainties of boundary conditions make Mode I degradation difficult to prove experimentally.

If the development of Poiseuille pressure causes the initiation stage of the degradation, a superimposed mechanical stress could modify the degradation process. In the present work, notched  $\beta''$ - $\text{Al}_2\text{O}_3$  and NaZrPSiO samples were electrolysed under stress. Subsequently, the fracture toughness

of the electrolysed samples was measured and the influence of both the magnitude and the sign of the superimposed stress on the degradation process was evaluated.

## 2. Experimental procedure

### 2.1. Sample preparation

MgO-stabilized Na- $\beta''$ -Al<sub>2</sub>O<sub>3</sub> samples were prepared with composition 11.10 wt% Na<sub>2</sub>O, 1.93 wt% MgO and the balance Al<sub>2</sub>O<sub>3</sub>. The chemicals, Al<sub>2</sub>(SO<sub>4</sub>)<sub>3</sub>, 18H<sub>2</sub>O, Na<sub>2</sub>CO<sub>3</sub> and MgSO<sub>4</sub> were carefully weighed and dissolved in distilled water. A fine jet of the solution was sprayed into liquid nitrogen and the resultant powder was freeze-dried for two days at 65° C. The powder was lightly milled, then calcined at 1320° C for 4 h. The calcine was then sieved, uniaxially pressed with 1 wt% binder and isostatically pressed at 340 MPa. The bar samples were pre-heated at 700° C and fired at 1600° C. The final sample composition by neutron activation energy analysis was 9.0 wt% Na<sub>2</sub>O, 2.1 wt% MgO and the balance Al<sub>2</sub>O<sub>3</sub>. Details of sample preparation have previously been reported [17, 18]. The samples were notched for toughness testing with a slow-speed diamond wheel.

### 2.2. Electrolysis and estimation of degradation

Two types of  $\beta''$ -Al<sub>2</sub>O<sub>3</sub>; MgO-stabilized Na- $\beta''$ -Al<sub>2</sub>O<sub>3</sub> made via the spray-freezing/freeze-drying technique (SF/FD sample) and Li<sub>2</sub>O-MgO-stabilized Na- $\beta''$ -Al<sub>2</sub>O<sub>3</sub> prepared by conventional techniques (ORF samples) and a NaZrPSiO were used in the present experiments. The characteristics of these samples are summarized in Table I. Notched beam samples were electrolysed at 280° C under applied stresses as shown in Fig. 1, i.e. (a) with zero-applied stress, (b) with a tensile stress at the notch tip, (c) with a compressive stress at the notch tip, and (d) with the sample under a uniaxial compressive stress orthogonal to the notch. Silver paint and NaNO<sub>3</sub>/NaNO<sub>2</sub> eutectic liquid were used as the negative and positive electrodes, respectively. Ca<sup>2+</sup> and K<sup>+</sup> impurities

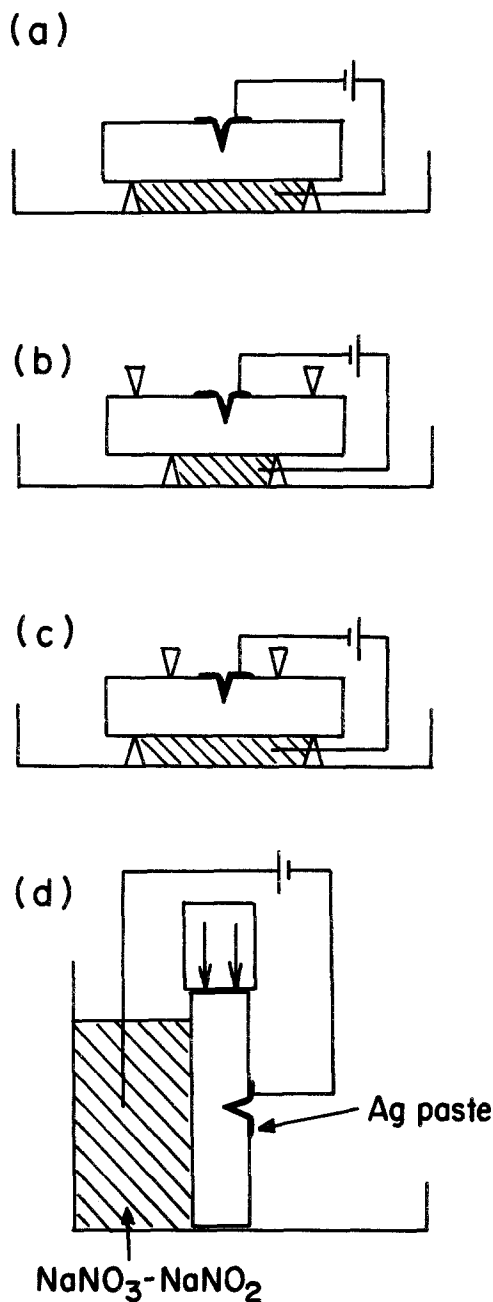


Figure 1 Notched beam samples electrolysed at 280° C with (a) zero-applied stress, (b) a tensile stress at the notch tip, (c) a compressive stress at the notch tip, and (d) the sample under a uniaxial compressive stress orthogonal to the notch.

TABLE I Physical properties and fabrication details of materials tested

Material	Fabrication	$f(\beta)$	Density (% theoretical)	Strength (MPa)	Grain size ( $\mu\text{m}$ )
MgO- $\beta''$ -Al <sub>2</sub> O <sub>3</sub>	SF/FD	0.18	99	280	0.2-2
Li <sub>2</sub> O/MgO- $\beta''$ -Al <sub>2</sub> O <sub>3</sub>	Conventional method	0.18	99	210	10
Na <sub>3,2</sub> Zr <sub>2</sub> Si <sub>2,2</sub> P <sub>0,8</sub> O <sub>12</sub>	Conventional method	-	92	85	-

in the eutectic were measured by atomic absorption as 6.0 and 3.5 ppm, respectively. To determine the current density in the vicinity of the notch tip, it alone was painted with silver paint and the sample conductivity measured. The negative electrode was then repainted and the conductivity remeasured. The conductivity difference gave the average current density in the vicinity of the notch tip. After electrolysis, samples were cleaned with methanol. The change of the critical fracture toughness parameter,  $K_{Ic}$ , of the samples before and after electrolysis was used to indicate the extent of electrolyte degradation\*.  $K_{Ic}$  was measured in four-point-bend at room temperature on a tensile machine with a cross-head speed of  $0.0508 \text{ cm min}^{-1}$ .  $K_{Ic}$  was calculated using the equation [19]

$$K_{Ic} = \frac{3P_f(L-l)}{2Bw^2} a^{1/2} \times \left[ 3.86 - 6.15 \left( \frac{a}{w} \right) + 21.7 \left( \frac{a}{w} \right)^2 \right]^{1/2}$$

where  $w$  is the sample height,  $B$  the sample width,  $a$  the notch length,  $L$  the major span,  $l$  the minor span and  $P_f$  is the applied load at fracture.

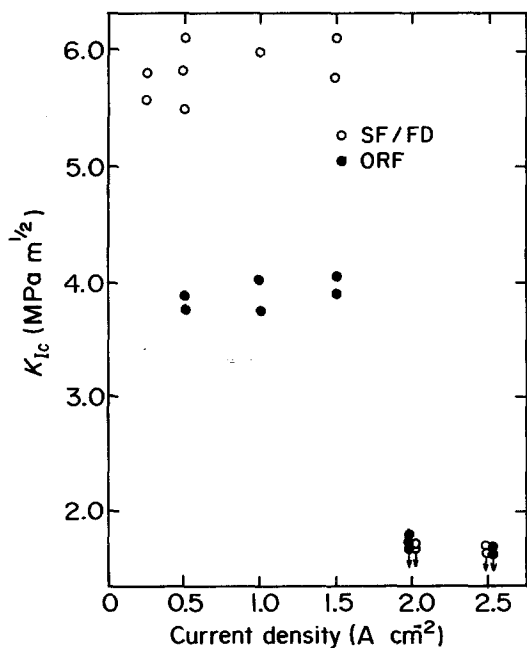


Figure 2  $\beta''$ - $\text{Al}_2\text{O}_3$  electrolysed under zero-load at  $280^\circ\text{C}$  for 30 min.

\*  $K_{Ic}$  measured after degradation is really an effective  $K_{Ic}$  as the crack length,  $a$ , has effectively increased as a result of the electrochemically-introduced damage.  $K_{Ic}$  will be used throughout the paper and its reduction is assumed to indicate increased flaw lengths.

### 3. Results and discussion

SF/FD and ORF samples were electrolysed at  $280^\circ\text{C}$  for 30 min under zero-applied stress conditions. Fig. 2 shows the variation of  $K_{Ic}$  with average notch-tip current-density. Both sample types did not degrade up to  $1.5 \text{ A cm}^{-2}$  but broke down within 10 min at current densities  $> 2.0 \text{ A cm}^{-2}$ . The ability to resist degradation appears independent of the initial strength of the sintered samples.

Samples were electrolysed under a tensile applied stress at  $280^\circ\text{C}$  for 30 min and Fig. 3 shows the  $K_{Ic}$  values of the electrolysed samples against the imposed-tensile stress at the notch tip. At a current density of  $0.30 \text{ A cm}^{-2}$  and up to  $150 \text{ MPa}$  tensile stress, no degradation was observed for either sample. Both sample types degraded within 30 min at  $0.5 \text{ A cm}^{-2}$  under  $120 \text{ (SF/FD)}$  and  $100 \text{ MPa (ORF)}$  tensile stress. At  $1.0 \text{ A cm}^{-2}$  SF/FD and ORF samples broke down when the tensile stress exceeded  $50 \text{ MPa}$ . The degradation rate increased with increasing tensile stress. These results suggest the degradation was enhanced by the superimposed tensile stress. Fig. 4 shows  $K_{Ic}$  against compressive stress at the notch tip in four-point-bend for samples electrolysed at  $280^\circ\text{C}$  for 30 min. Compressive stress at the notch tip should counter developing Poiseuille pressure. However, both SF/FD and ORF samples broke down at  $1 \text{ A cm}^{-2}$  for compressive stresses  $> 75 \text{ MPa}$ . The degradation rate increased with increasing applied compressive stress.

ORF samples were electrolysed under  $50 \text{ MPa}$  of uniaxial compressive stress at  $280^\circ\text{C}$  for 30 min. At a current density of  $1.5 \text{ A cm}^{-2}$ , one sample broke down but two samples were not degraded. All three samples broke down at  $2.0 \text{ A cm}^{-2}$ . Even a uniaxial compressive stress on the sample did not arrest degradation.

The same tendencies were observed for the NaZrPSiO samples. This material failed in  $< 5 \text{ min}$  for current densities  $> 0.5 \text{ A cm}^{-2}$ . Fig. 5 shows  $K_{Ic}$  against average current density (up to  $0.5 \text{ A cm}^{-2}$ ) for NaZrPSiO, electrolysed under zero-load and  $30 \text{ MPa}$  of uniaxial compression. The longer time involved in these tests was dictated by the degradation kinetics at these current densities. In both cases, the NaZrPSiO degraded after 120 min

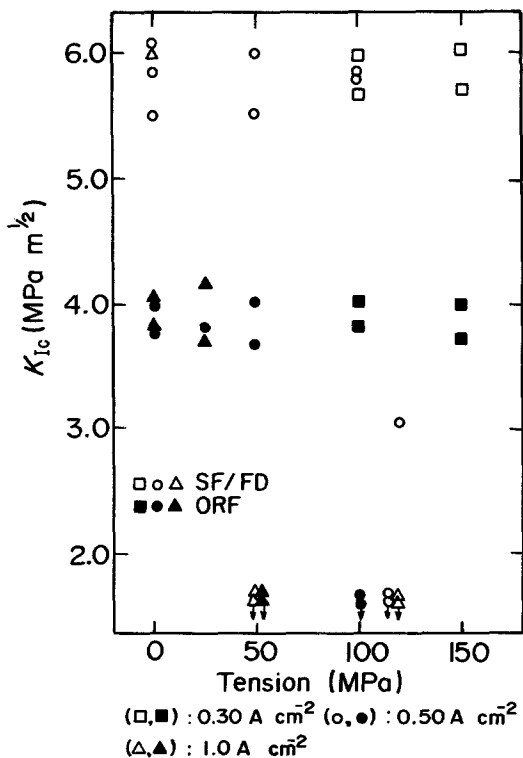


Figure 3 SF/FD and ORF samples electrolysed under tensile stress at  $280^\circ \text{C}$  for 30 min.

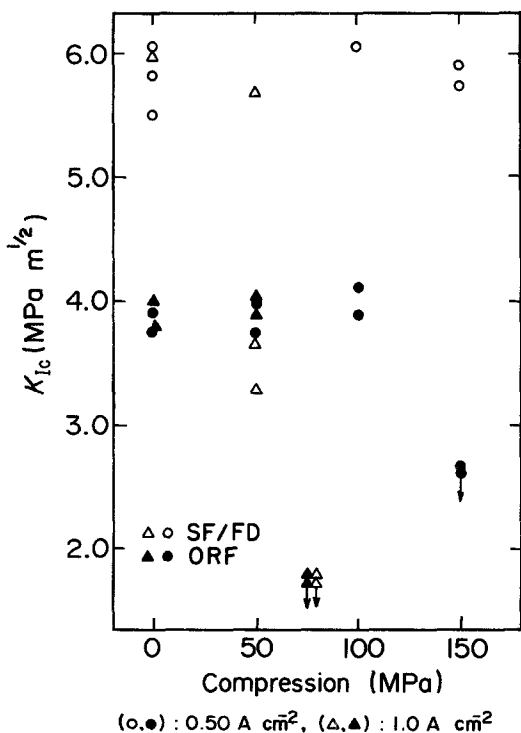


Figure 4 SF/FD and ORF samples electrolysed under compression stress at  $280^\circ \text{C}$  for 30 min.

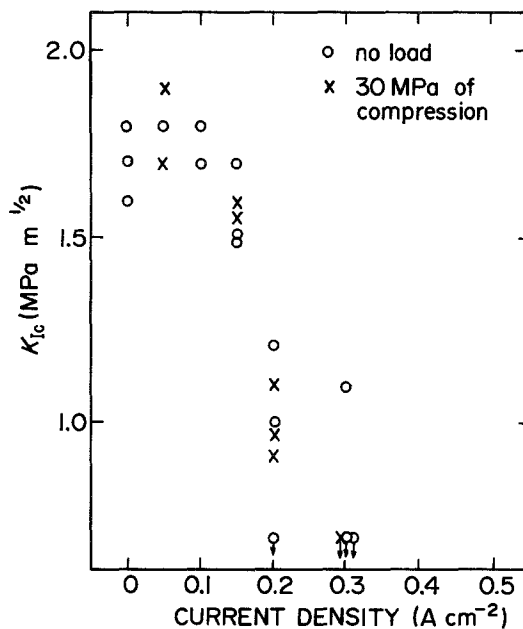


Figure 5 NaZrPSiO electrolysed at  $280^\circ \text{C}$  for 20 min.

at current densities  $> 0.20 \text{ A cm}^{-2}$ . Clearly uniaxial compressive stress does not prevent electrolyte degradation.

The kinetics of stress-enhanced degradation of the notched samples were then investigated. Having determined that SF/FD  $\beta''\text{-Al}_2\text{O}_3$  survived  $> 24 \text{ h}$  under a current density of  $0.3 \text{ A cm}^{-2}$  at  $280^\circ \text{C}$  and zero tensile stress, it was subjected to  $0.3 \text{ A cm}^{-2}$  with  $150 \text{ MPa}$  tensile stress at the notch tip over a range of temperatures. NaZrPSiO, which survived  $> 24 \text{ h}$  at  $280^\circ \text{C}$  under  $0.02 \text{ A cm}^{-2}$  and zero applied stress was electrolysed at  $0.02 \text{ A cm}^{-2}$  with  $30 \text{ MPa}$  tensile stress at the notch tip over the same temperature range. The total stress at flaw tips in each case is that developed by the Poiseuille pressure plus the concentrated applied stress. Keeping the latter constant, the Poiseuille pressure contribution will vary with temperature, as it is proportional to the viscosity of liquid sodium. Degradation was, however, enhanced at higher temperatures and the influence of temperature on the time-to-failure ( $t_f$ ) is shown in Fig. 6. At constant stress,  $\log(1/t_f)$  varies linearly with  $(1/T)$  giving apparent activation energies of  $27.6 \text{ kJ mol}^{-1}$  for SF/FD and  $31.0 \text{ kJ mol}^{-1}$  for NaZrPSiO, respectively. These values are close to those for diffusion of  $\text{Na}^+$  in the SF/FD  $\beta''\text{-Al}_2\text{O}_3$  [18] ( $20.9 \text{ kJ mol}^{-1}$ ) and the  $\text{Na}_{3.2}\text{Zr}_2\text{Si}_{2.2}\text{P}_{0.8}\text{O}_{12}$  [20] ( $23.0 \text{ kJ mol}^{-1}$ ). This agreement suggests that  $\text{Na}^+$  dif-

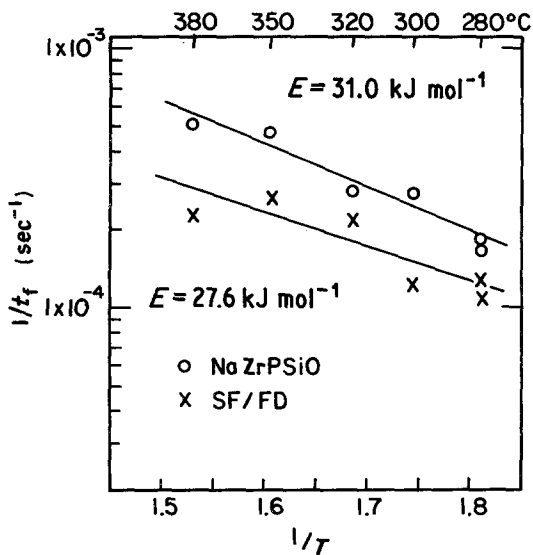


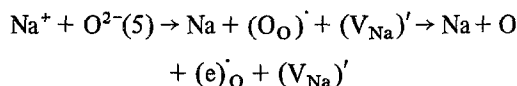
Figure 6 Influence of temperature on time-to-failure for SF/FD and NaZrPSiO electrolysed under tensile stress.

fusion is controlling the rate of degradation of both materials.

According to Davidge *et al.* [7]  $\beta$ -Al<sub>2</sub>O<sub>3</sub> is not degraded under stress without current flow. Shetty *et al.* [6] also found zero stress corrosion of  $\beta''$ -Al<sub>2</sub>O<sub>3</sub> after immersion in liquid sodium. The ceramic is discoloured by immersion in liquid sodium however, even when no current is passed. Other observations pertinent to the discoloration process are: transmission electron microscopy failed to identify the defects causing the blackening [11]; careful polishing of the darkened material revealed it to be a deep violet [21]; sodium colloids, microcracks and some macrocracks were determined after extended service life [13]; high resolution electron microscopy showed the destruction of conduction layers in  $\beta$ -Al<sub>2</sub>O<sub>3</sub> and the "sweating" of sodium metal from the foils [22–25]. Gourier and Wicker [26] examined blackened electrolytes by electron spin resonance (ESR). They detected a C-centre corresponding an unpaired electron bonded at a lattice site in the aluminate structure and a D-centre interpreted as colloidal sodium of 1  $\mu$ m diameter. The blackening of ZrO<sub>2</sub> at high current densities is also associated with the reduction of the oxide to colloidal Zr [27]. De Jonghe *et al.* [11] noted that the cathode of a dog-bone shaped sample turned black and sodium metal was detected inside the grains and along the grain boundaries in the vicinity. Blackening was not observed in the narrow section of the sample even at 10 A cm<sup>-2</sup>. On this basis it was concluded

that electron injection was necessary to produce discolouration. However many workers have reported the blackening of  $\beta$ -Al<sub>2</sub>O<sub>3</sub> in sodium with no current passage. This and further evidence led De Jonghe *et al.* [13] to suggest two modes of degradation i.e. Mode I, which is Poiseuille pressure originated and Mode II, in which blackening is associated with local oxidation of oxygen ions in the  $\beta$ -Al<sub>2</sub>O<sub>3</sub> structure and the production of colour centres therein. The following specific process development extends De Jonghe's interpretation. The feasibility of the proposed mechanism is demonstrated in a companion paper [28].

As reported by De Jonghe *et al.* [11] current flow in  $\beta/\beta''$ -Al<sub>2</sub>O<sub>3</sub> is inhomogeneous. Local current focusing into a few grains in the vicinity of surface cracks could occur via the anisotropic microstructure. Sodium-filled surface cracks must also enhance the current focusing. Since the number of conduction planes in the few suitably orientated grains into which the sodium is focused is significantly less than the number which carried the Na<sup>+</sup> through the electrolyte section before focusing, local saturation of Na<sup>+</sup> is possible adjacent to the focusing grains. This saturation of Na<sup>+</sup> could "overload" the available discharge "channels" and sodium atoms might precipitate, capturing the requisite electrons from local oxygen (5) ions, O(5) is the conduction-plane oxygen position). Such a mechanism could result from two reactions:



The oxygen atoms produced will form Na<sub>2</sub>O in air [29] and escape as O<sub>2</sub> in vacuum. The second reaction would explain the observation of colour centres, (e<sub>O</sub>)<sup>·</sup> (violet colour) and free electrons on aluminate sites via ESR. The production of V'<sub>Na</sub> would also allow the non-precipitated Na<sup>+</sup> to discharge into the sodium-filled flaws. The second reaction must involve eventual collapse of the conduction plane as the O(5) ions are removed. Darkened electrolyte can maintain its ionic conductivity so initial removal of O(5) does not induce collapse. Above a critical current density however conduction planes will close and accelerated degradation will result. In both reactions sodium is produced. These observations agree with the high resolution electron microscopic observations of conduction plane disappearance and sodium metal colloid production. The initial

colour centres and sodium atoms would not be detectable by TEM but eventual condensation of the sodium into colloids would render detection possible. The formation of sodium or Na<sub>2</sub>O colloids on grain boundaries and within grains in a dense microstructure would produce microcracks and these will allow further sodium precipitation. These in turn could join with the major focusing flaws so giving apparent sodium "dendrite" growth into the electrolyte from the sodium electrode side, as observed. This progression suggests that Mode I and II deterioration are sequential with the sequence the reverse of that suggested by De Jonghe.

An applied compressive stress would enhance the sodium precipitation by lowering the structural back stress resisting sodium precipitation on those grain boundaries parallel to the stress axis. Such boundaries being perpendicular to the active sodium-transporting flaws will be blocking to Na<sup>+</sup> transport making them likely precipitation sites. An applied tensile stress would promote sodium-precipitation on grain boundaries parallel to the sodium-metal-transporting flaws, i.e. these grains and boundaries being perpendicular to the applied stress axis will resist precipitation with a lower back stress as a result of the applied tensile stress. Such a precipitation will effectively extend the sodium-penetration of the ceramic. Hence stress of either sign will enhance the ceramic degradation.

The precipitation reactions quoted are not rate-controlling, as the observed activation energies are those for Na<sup>+</sup> diffusion. This observation is addressed in detail in a companion paper and diffusion control of the process is demonstrated [28]. The fact that NaZrPSiO degrades in a similar fashion suggests that its three-dimensional channels for Na<sup>+</sup> transport can also be saturated and sodium metal precipitated. The higher anisotropy of β''-Al<sub>2</sub>O<sub>3</sub> will accentuate the process but its higher mechanical strength will give backstresses that resist sodium precipitation to higher current densities. The role of the morphological differences between β''-Al<sub>2</sub>O<sub>3</sub> and NaZrPSiO is clear in the pattern of blackening observed by Virkar and Viswanathan [29]. The blackening of β''-Al<sub>2</sub>O<sub>3</sub> was localized, whereas it was uniform across the section of NaZrPSiO.

One vital area not discussed in the present paper is the role of impurities in the degradation process. Of particular concern are K<sup>+</sup>, Ca<sup>2+</sup>, Si<sup>4+</sup> and H<sub>3</sub>O<sup>+</sup>. These are presently under investigation.

Much has been reported on the degradation of sodium superionic conductors and in some cases Mode I failure was observed without the precursing Mode II. The damaging potential of impurity ions may explain these observations.

#### 4. Summary

Notched beam β''-Al<sub>2</sub>O<sub>3</sub> and NaZrPSiO samples were electrolysed at 280°C under applied compressive and tensile stresses and the mechanisms of electrolyte degradation studied. Both tensile and compressive stress at the notch enhanced the degradation process. The influence of temperature on the degradation of electrolytes under tensile stress was also studied. Degradation was enhanced at higher temperatures. The apparent activation energy was estimated as 27.6 kJ mol<sup>-1</sup> for β''-Al<sub>2</sub>O<sub>3</sub> and 31.0 kJ mol<sup>-1</sup> for NaZrPSiO between 280 and 380°C. An electrochemical stress corrosion model is proposed to explain the degradation process. The degradation behaviour under compressive and tensile stresses and increased temperatures militates against the Poiseuille pressure model as the degradation mechanism.

#### Acknowledgements

The authors are indebted to S. Kamenshchik for her assistance. Appreciation is also extended to R. Roy of Ontario Research Foundation.

#### References

1. I. YASUI and R. H. DOREMUS, *J. Amer. Ceram. Soc.* **60** (1977) 296.
2. *Idem*, *J. Electrochem. Soc.* **125** (1978) 1007.
3. R. D. ARMSTRONG, T. DICKINSON and J. TURNER, *Electrochimica Acta* **19** (1974) 187.
4. R. H. RICHMAN and G. J. TENNENHOUSE, *J. Amer. Ceram. Soc.* **58** (1975) 63.
5. G. J. TENNENHOUSE, R. C. KU, R. H. RICHMAN and T. J. WHALEN, *Amer. Ceram. Soc. Bul.* **54** (1975) 523.
6. D. K. SHETTY, A. V. VIRKAR and R. S. GORDON, *Fract. Mech. Ceram.* **4** (1978) 651.
7. R. W. DAVIDGE, G. TAPPIN, J. R. McLAREN and G. J. MAY, *J. Amer. Ceram. Soc.* **58** (1979) 771.
8. C. A. WORRELL and B. A. W. REDFERN, *J. Mater. Sci.* **13** (1978) 1515.
9. N. K. GUPTA and G. J. TENNENHOUSE, *J. Electrochem. Soc.* **126** (1979) 145.
10. M. P. J. BRENNAN, *Electrochim. Acta.* **25** (1980) 629.
11. L. C. DE JONGHE, L. FELDMAN and P. MILLET, *Mater. Res. Bull.* **14** (1979) 589.
12. L. C. DE JONGHE and L. FELDMAN, *ibid.* **15** (1980) 777.

13. L. C. DE JONGHE, L. FELDMAN and A. BEUCHELE, *J. Mater. Sci.* **16** (1981) 780.
14. A. V. VIRKAR, L. VISWANATHAN and D. R. BISWAS, *ibid.* **15** (1980) 302.
15. A. V. VIRKAR, *ibid.* **16** (1981) 1142.
16. D. S. DEMOTT, *J. Electrochem. Soc.* **127** (1980) 2312.
17. A. PEKARSKY and P. S. NICHOLSON, *Mater. Res. Bull.* **15** (1980) 1517.
18. K. KURIBAYASHI and P. S. NICHOLSON, *ibid.* **15** (1980) 1595.
19. J. L. HENSHALL, D. J. ROWCLIFFE and J. W. EDINGTON, *J. Mater. Sci.* **19** (1974) 1559.
20. J. B. GOODENOUGH, H. Y-P. HONG and J. A. KAFALAS, *Mater. Res. Bull.* **11** (1976) 203.
21. J. R. RASSMUSSEN, G. R. MILLER and R. S. GORDON, Annual Convention of the Electrochemical Society, Montreal, May 1982. Abstract no. 720.
22. J. O. BOVIN, *Nature* **273** (1978) 136.
23. J. O. BOVIN, "Fast Ion Transport in Solids", edited by Vashishta, Mundy and Shenoy, (Elsevier North Holland Inc., Amsterdam and New York, 1979) p. 315.
24. T. B. TANG, G. ABRAMSON and M. M. CHANDHRI, *Sol. Stat. Ionics* **3/4** (1981) 397.
25. Y. MATSUI, *ibid.* **3/4** (1981) 135.
26. D. GOURIER and A. WICKER, Annual Convention of the Electrochemical Society, Montreal, May 1982. Abstract No. 722.
27. P. FABRY, M. KLEITZ and C. DEPORTES, *J. Solid State Chem.* **6** (1973) 230.
28. P. S. NICHOLSON, *J. Mater. Sci.* submitted.
29. A. V. VIRKAR and L. VISWANATHAN, *J. Amer. Ceram. Soc.* **62** (1979) 528.

*Received 20 May  
and accepted 31 August 1982*